Surface Oxygen Diffusion into Neutral, Cationic, and Dicationic Oxygen Vacancies on MgO(100) Surfaces

ARTICLE *in* THE JOURNAL OF PHYSICAL CHEMISTRY C · JUNE 2010

Impact Factor: 4.77 · DOI: 10.1021/jp1040184

4 AUTHORS, INCLUDING:

Jose Ulises Reveles
Virginia Commonwealth University
76 PUBLICATIONS **1,429** CITATIONS

SEE PROFILE

Carlos Quintanar
Universidad Nacional Autónoma de México
23 PUBLICATIONS **141** CITATIONS

SEE PROFILE

Surface Oxygen Diffusion into Neutral, Cationic, and Dicationic Oxygen Vacancies on MgO(100) Surfaces

J. Ulises Reveles,*,† Andreas M. Köster,‡ Shiv N. Khanna,† and Carlos Quintanar§

Physics Department, Virginia Commonwealth University, Richmond, Virginia 23284-2000, Departamento de Química, Cinvestav, Avenida Instituto Politécnico Nacional 2508, A.P. 14-740, México, D.F., 07000, México, and Facultad de Ciencias, Universidad Nacional Autónoma de México, Ciudad Universitaria, 04510 México, D.F., México

Received: May 3, 2010; Revised Manuscript Received: June 1, 2010

First principles electronic structure investigations of the oxygen diffusion into neutral, cationic, and dicationic oxygen vacancies on MgO(100) surfaces have been carried out within a density functional theory cluster-embedding approach. The transition states and activation barriers for the oxygen diffusion were determined. It was found that the charge of the vacancy has a marked effect on the oxygen diffusion as the activation barrier decreases from 2.84 eV in the neutral, to 2.18 eV in the cationic, and to 0.94 eV in the dicationic oxygen vacancies. An analysis of the relaxation of the surface atoms around the vacancies, and the geometry of the transition states, leads us to conclude that the attractive interaction between the localized positive charge and the electron-rich oxygen atoms, and the relaxation of surface atoms, are responsible for lowering the activation barrier. In addition, our studies on layer relaxations indicate that the oxygen diffusion is strongly confined to the surface atoms. The analysis of the spin density along the reaction path of the oxygen diffusion into a cationic vacancy suggests that the oxygen movement is accompanied by an electron hopping process.

1. Introduction

Developments in experimental techniques are enabling the tuning of metal oxide structure and the nature of defects and their concentration, thus opening new avenues for a variety of advanced technological applications, i.e., corrosion protection, coating for thermal application, heterogeneous catalysis, magnetic recording devices, and high temperature fuel cells.[1–3] Depending on the experimental treatment of the sample, materials with a variety of defects, which deviate from ideal stoichiometry, can be generated. These defects include morphological irregularities such as surface steps, impurities or dopant atoms, and neutral or ionic vacancies[4–6] and are known to have an important role in the structural properties[2] and the catalytic activity of oxide surfaces.[7,8] For example, the oxygen vacancy sites (F centers) trap electron charges and hence can promote catalysis through electron transfer. In fact, Köning et al.[9] have recently used frequency modulated dynamic force microscopy (FM-DFM) and scanning tunneling microscopy (STM) to image charge defects in MgO films (3−6 layers) on a Ag(001) surface. Their results show how the neutral F^0, cationic F^+, and dicationic F^{2+} centers localize charge at the defect sites. The vacancy sites with one (F^+) and two trapped electrons (F^0) have also been shown to facilitate the growth of Pd clusters on MgO surfaces and to promote their catalytic activity by enhancing the charge transfer from the surface to the adsorbed cluster.[10,11] Similarly, the transfer of one electron from a vacancy site on an MgO surface to an adsorbed N_2 molecule has experimentally and theoretically been shown to form the N_2^- radical anion, which can be seen as a first step toward the process of nitrogen fixation.[8]

The role of the oxygen vacancies, however, is not limited to enhancement of charge transfer but also has a dynamical aspect essential to chemical reactions. For example, oxide surfaces can generate vacancies by providing oxygen atoms for the oxidation of deposited organic substrates. Gas-phase O_2 molecules then dissociate at the vacancy sites to regenerate the surface and to form highly reactive O atoms on the surface.[12] An investigation of the processes leading to the formation and dynamics of neutral and cationic oxygen vacancies is thus important. For both MgO bulk and single crystals, the oxygen vacancy has been predicted to involve large formation energies of around 9 eV,[13–15] and experimental studies on the diffusion of vacancies in the bulk,[16–19] and theoretical studies on MgO surfaces,[20–25] have estimated large diffusion energy barriers in the order of 2−3 eV.

In this study we present a comprehensive investigation of the oxygen diffusion in neutral, cationic, and dicationic oxygen vacancies on a MgO(100) surface employing a density functional theory (DFT) cluster-embedding approach. In particular we delineate the role of charging and the relaxation of atoms on the energy barriers. This real-space approach adapted for free clusters is well suited to investigate charged systems. This is in sharp contrast to methods using supercells where charged species lead to nonphysical interactions and uncontrolled artifacts within the repeated unit cells.[25] As the supercell is the most commonly employed method for the investigation of metal oxide surfaces, the lack of an appropriate way to treat ionic systems has limited the study of oxygen diffusion on cationic oxygen vacancies, although they are clearly of great interest.

In the present study the transition states and activation barriers for the oxygen diffusion are determined, and the effect of the vacancy charge on these barriers is analyzed. We compare our calculated activation barriers with available experimental data in bulk[16–19] and theoretical studies on MgO surfaces.[20–25] Further, we investigate the effect of the number of layers and the

* Corresponding author. E-mail: jureveles@vcu.edu.
† Virginia Commonwealth University.
‡ Cinvestav, México.
§ Universidad Nacional Autónoma de México.

10.1021/jp1040184
Published on Web 06/29/2010

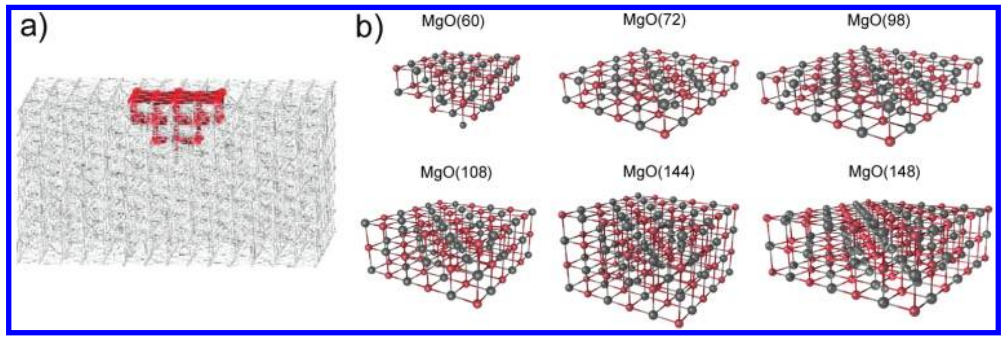

Figure 1. (a) Embedded $Mg_{30}O_{30}$ cluster. The cluster is centered at an oxygen site of the MgO(100) surface, and the embedding consists of 1740 point charges. (b) MgO cluster models studied. The total number of Mg and O atom is given in parentheses.

TABLE 1: Relaxation and Rumpling for the MgO Cluster Models Shown in Figure 1b[a]

	MgO(60)25,25,9,1	MgO(72)36,36	MgO(98)49,49	MgO(108)36,36,36	MgO(144)36,36,36,36	MgO(148)49,49,49,1
R_1	2.131	2.132	2.134	2.118	2.135	2.139
R_2	2.109	2.093	2.097	2.140	2.116	2.118
$\Delta(R_1 - R_2)$	0.023	0.038	0.037	0.022	0.020	0.022

[a] The number in parentheses indicates the total number of Mg and O atoms. The sequence of numbers indicates the number of atoms in each layer. R_1 and R_2 correspond, respectively, to the O−Mg and Mg−O bond distance between the first sublayer and the MgO surface. Bond lengths are in units of angstroms.

relaxation of the inner layers on the activation barriers. Finally, we analyze the movement of the unpaired electron in the cationic oxygen vacancy during the oxygen diffusion through plots of the spin density along the reaction path.

2. Methods

A. Cluster Embedded Model. The essential features of the cluster embedding technique used in this study are illustrated in Figure 1a.[26] In this method the active cluster, i.e., $Mg_{30}O_{30}$ shown in red color, is treated within a first principles DFT calculation. To provide a proper electrostatic environment and boundary conditions, an Evjen array of 1740 point charges surrounds the active cluster so as to form a MgO(100) surface. This embedding model has been previously used for the calculation of the relaxation and rumpling of the MgO(100) surface[27,28] and the adsorption of gold atoms and dimers on this surface.[28] In the present study, we investigate the MgO cluster models containing 60, 72, 98, 108, 144, and 148 atoms as shown in Figure 1b. In each case the DFT cluster models were surrounded by point charges such that the total number of centers, i.e., DFT atoms and point charges, sum to 1800. For each MgO cluster the bottom layers were fixed at the experimental bulk position (R_{MgO} = 2.105 Å),[29] and the relaxation and rumpling of the surface atoms were calculated using a combination of equivalent and constrained optimization schemes as described in a previous work.[28] A good agreement was found between the different clusters when optimizing the equivalent coordinates R_1 (R_2), representing the bond length between an oxygen (magnesium) on the surface, and a magnesium (oxygen) in the first sublayer as shown in Table 1, validating the models used to study the MgO surface. In the present study we have chosen the 144 atom MgO cluster named MgO(144) composed of four layers of 36 atoms (Figure 1b and Table 1). This cluster is large enough to model the oxygen atom diffusion on the MgO surface into neutral vacancies as shown in a recent work using supercells by Carrasco et al.[25] Additional calculations were conducted to investigate the effect of the inner layer relaxation and of the cluster thickness on the oxygen diffusion energy barrier. For these calculations we used clusters with three and two layers where each layer consists of 36 atoms, to form respectively, the MgO(108) and MgO(72) clusters shown in Figure 1b. In addition, to study the effect of the local layer relaxation on the oxygen energy barrier, the two topmost surface layers of the MgO(144) and MgO(108) cluster models were relaxed.

B. Quantum Chemical Methods. All calculations were performed within a spin-polarized DFT formalism employing the Perdew, Burke, and Enzerhof generalized gradient approximation (GGA).[30] The molecular orbitals and eigenstates were determined by using a linear combination of Gaussian type orbital expansion. The numerical calculations were carried out using the deMon2k software.[31] A variational fitting of the Coulomb potential was employed in order to avoid the calculation of four-center electron repulsion integrals.[32] An auxiliary density functional theory method was used in which the exchange-correlation potential is calculated via a numerical integration from the auxiliary function density.[33] All electrons of the MgO cluster were treated explicitly using the double-ζ valence plus polarization (DZVP) basis sets (6321/411/1*) for magnesium and (621/41/1*) for oxygen,[34] and the GEN-A2 auxiliary function set.[35] For the geometry optimization, a quasi-Newton method in delocalized internal coordinates was used.[36] Equivalent and constrained coordinates are formulated in terms of these coordinates.[37] For the local transition state search, an uphill restricted step method with eigenvector following was employed.[38] The above-defined theoretical method has been successfully used for the calculation of the rumpling and relaxation of the MgO(100) surface.[27,28] In addition, we calculated the formation energy of the neutral vacancy site in the MgO(144) cluster, defined as the energy required to remove an O atom in its triplet state ($^3P_2$) from the MgO surface. Our calculated value of 9.01 eV is in good agreement with previous calculations employing periodic cell methods[13,15] (9.02 and 9.06 eV), as well as an embedded cluster method[14] (9.07 eV).

3. Results and Discussion

A. Optimized MgO Cluster with Neutral, Cationic, and Dicationic Oxygen Vacancies. The MgO(144) cluster was optimized for the neutral, cationic, and dicationic oxygen vacancies. The perspective (whole cluster) and top views (of the surface layer) of the final geometry for the neutral vacancy are shown in Figure 2. We have optimized the Mg and O atoms

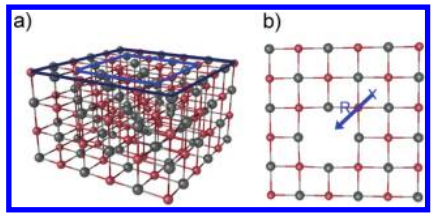

Figure 2. Perspective view (whole cluster) (a) and top view (surface layer) of the MgO(144)-optimized geometry of a neutral vacancy (b). The large and small squares marks the two sets of MgO atoms that were optimized (see text for details). The arrow describes the oxygen diffusion path along the coordinate R. The X marks a reference point.

of the surface layer grouped in two sets to provide proper boundary conditions and to allow full relaxation around the vacancy site. The first group consists of the 20 edge atoms marked with a large black square in Figure 2a. These atoms are optimized only along the direction perpendicular to the surface employing two sets of equivalent coordinates that correspond to the R_1 (O−Mg) and R_2 (Mg−O) bond lengths, respectively. The second group consists of the 15 atoms enclosed in the small blue square in Figure 2a. These atoms are fully optimized in all directions.

It was found that the surface atoms around the cationic and dicationic vacancies presented a significantly larger distortion compared with the neutral vacancy structure. Upon optimization, the Mg ions moved outward with respect to the vacancy site with a stretching of the Mg-vacancy bond length with respect to the stoichiometric surface without vacancies by 2.1%, 6.4%, and 11.0% for the neutral, cationic, and dicationic vacancies, respectively. On the other hand, the neighboring oxygen atoms relaxed toward the vacancy with a shrinking of the O-vacancy bond length by 0.4%, 2.6%, and 6.7%, respectively. These results are in good agreement with a previous theoretical study of neutral and cationic vacancies employing a Hartree−Fock cluster embedding approach by Ferrari and Pacchioni.[39] The differences in the relaxation of the geometries for various charged cases can be explained by the attractive electrostatic interaction between the localized positive charge and the electron-rich oxygen atoms, and it is discussed later in this paper as a relevant factor that significantly lowers the oxygen diffusion energy barriers into the cationic and dicationic vacancies.

B. Surface Oxygen Diffusion into a Neutral Vacancy. The reaction energy path was calculated for the diffusion of an oxygen atom from an adjacent diagonal site toward the neutral vacancy site. We performed a constraint optimization of the oxygen atom along the coordinate R shown in Figure 2b. The oxygen atom was allowed to move on the surface and in the perpendicular direction to explore the possible diffusion paths. The calculated energy path presented a maximum (an approximation of the transition state) that corresponds to an activation barrier of 2.84 eV.

Our approximated activation barrier is in fair agreement with a previous semiemprirical INDO study by Popov et al.[21] that predicts a value of 3.13 eV, in good agreement with an LDA study by Finochi et al.[24] with a value of 2.6 eV and in even closer agreement to a GGA study by Carrasco et al. with a value of 2.69 eV.[25] Experimentally, the estimated diffusion energy barrier for bulk MgO presents a broad range of values ranging from 1.95 eV[16] to 3.4 eV.[19] This dispersion of values has been attributed to the experimental difficulty in measuring the energy barriers, as under the sample annealing conditions there exist other processes competing with the oxygen diffusion. To the best of our knowledge there exist no corresponding measurements of activation barriers on the MgO(100) surface; therefore, the bulk activation barriers are used as a reference.

TABLE 2: Activation Barriers for the Diffusion of an Oxygen Atom into a Neutral, a Cationic, and a Dicationic Oxygen Vacancy on the MgO(100) Surface[a]

cluster model	surface layer optimized	two layers optimized	local TS search
Neutral Vacancy			
four layer MgO(144)	2.84	2.89	
three layer MgO(108)	2.91	2.82	
two layer MgO(72)	2.86		2.86
Cationic Vacancy			
four layer MgO(144)	2.18	2.19	
three layer MgO(108)	2.22	2.18	
two layer MgO(72)	2.17		2.17
Dicationic Vacancy			
four layer MgO(144)	0.94	1.01	
three layer MgO(108)	0.95	1.02	
two layer MgO(72)	0.91		0.91

[a] All values are in units of eV.

In our next step we investigated the effect of layer thickness on the activation barriers. For this purpose, we first calculated an MgO(108) cluster composed of three layers of 36 atoms (Figure 1b). In this cluster the lowermost layer of the MgO(144) cluster is substituted by point charges that add to the embedding cube. Second, we calculated an MgO(72) cluster composed of only two layers of 36 atoms (Figure 1b). In this case the two lowermost layers of MgO(144) are substituted by point charges. The energy profiles and approximated activation barriers were calculated as described before. We found approximate activation barriers of 2.91 and 2.86 eV for the MgO(108) and MgO(72) cluster, respectively. These results show that the activation barrier does not depend on the MgO cluster thickness, and that the oxygen diffusion is a phenomenon well localized at the MgO surface.

Following this, we investigated the effect of the relaxation of the layer below the surface on the activation barrier. We repeated our study with the MgO(144) and MgO(108) clusters, now optimizing the two topmost MgO surface layers. The calculated barriers were 2.89 and 2.82 eV, respectively, in good agreement with the studies in which only the topmost layer was optimized. This result shows again that only the topmost layer is affected by the oxygen diffusion. All calculated activation barriers are collected in Table 2. To further confirm the nature of the maximum along the reaction path, we investigated in more detail the MgO(72) cluster. Starting from the geometry of the energy path maximum, the transition state (TS) geometry was located and characterized by a frequency analysis. The optimized TS geometry is shown in Figure 3a. This transition state corresponds to a diffusion energy barrier of 2.86 eV, attesting to the validity of our constraint optimization technique and the accuracy of the approximated activation barriers.

C. Surface Oxygen Diffusion into a Cationic Oxygen Vacancy. The reaction energy path was calculated in the MgO(144) cluster for the diffusion of oxygen toward a cationic vacancy in a way similar to that described above for the neutral vacancy. The calculated energy path presented a maximum that corresponds to a diffusion energy barrier of 2.18 eV. For single cationic vacancies, a number of semiempirical INDO calculations by Popov et al.[19] predict an activation barrier of 2.72 eV. The experimental activation energy for the single cationic vacancy is not well established and its value has been estimated to be roughly around 3 eV.[22]

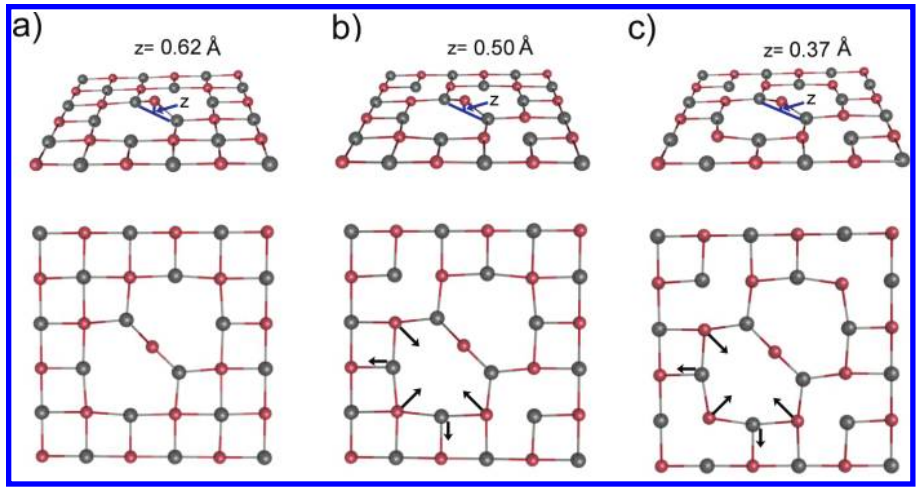

Figure 3. Perspective and top view of the surface layer for the MgO(72) transition state geometries for the diffusion of oxygen atoms into neutral (a), cationic (b), and dicationic (c) vacancies. The arrows indicate the direction of the movement of O and Mg atoms during the geometry optimization. The z value denotes the height of the moving oxygen above the MgO surface.

An investigation of the effect of cluster thickness on the activation barrier was also conducted in this case. The energy profile and approximated activation barriers were calculated to be 2.22 and 2.17 eV, respectively, for the MgO(108) and MgO(72) clusters. These results show that, as in the case of the neutral vacancy, the oxygen diffusion is confined to the MgO surface, and the activation barrier does not depend on the MgO cluster thickness. Similarly, studies conducted on the relaxation of the layer below the surface with the MgO(144) and MgO(108) clusters optimizing the two topmost layers produced barriers of 2.19 and 2.18 eV, again confirming, as in the neutral vacancy case, that the oxygen diffusion only impacts the MgO surface structure. All calculated activation barriers for the cationic oxygen vacancy are collected in Table 2. To confirm the nature of the maximum along the reaction path, an exact transition state was located starting from the geometry of the energy path maximum of the MgO(72) cluster and characterized by a frequency analysis. The transition state geometry shown in Figure 3b corresponded to an activation barrier of 2.17 eV, again in excellent agreement with our approximated activation energy.

For a vacancy with two positive charges, Pacchioni and Pescamora predicted an upper bound to the energy barrier of 1.58 eV using a Hartree−Fock cluster model approach.[23] They also concluded that higher barriers were expected for neutral or singly charged vacancies because of the repulsion of the migrating O ions with the trapped electrons. To further rationalize the lowering of the energy barrier with respect to the neutral case, we investigated the effect of the surface relaxation. To this end, we performed additional calculations of the energy profile having frozen the geometry of the MgO(72) cluster at the optimized geometry of both the neutral and cationic vacancies. For the neutral vacancy, the estimated energy barrier did not change from the 2.86 eV calculated for the fully relaxed case, in agreement with the small surface relaxation observed for this case. Surprisingly, the energy barrier calculated for the cationic vacancy increased with respect to the relaxed case to 2.72 eV. This implies that the surface relaxation is able to decrease the energy barrier by 0.55 eV to the actual value of 2.17 eV for the fully relaxed case.

The fact that the MgO surface with the cationic vacancy presents significantly larger distortions with the oxygen atoms optimizing toward and the Mg atoms away from the vacancy site, respectively, lead us to conclude that the electrostatic interaction between the localized positive charge and the electron-rich oxygen atoms, and the surface relaxation, are the driving forces for lowering the oxygen diffusion energy barrier.

D. Surface Oxygen Diffusion into a Dicationic Oxygen Vacancy. The reaction energy path was calculated in the MgO(144) cluster for the diffusion of oxygen toward a dicationic vacancy in a way similar to that described above for the neutral and cationic vacancies. The calculated energy path shows a maximum that corresponds to an approximate diffusion energy barrier of 0.94 eV. This result is consistent with a Hartree−Fock cluster embedding study by Pacchioni and Pescamora that predicted an upper bound of 1.58 eV to the actual energy barrier.[23]

An investigation of the effect of cluster thickness on the activation barrier led to energy profiles and approximated activation barriers of 0.95 and 0.91 eV for the MgO(108) and MgO(72) clusters, respectively. Similar studies conducted on the relaxation of the two topmost layers for the MgO(144) and MgO(108) clusters predicted barriers of 1.01 and 1.02 eV, respectively. All calculated activation barriers are collected in Table 2. These results confirm, as in the neutral and cationic vacancy cases, that the oxygen diffusion only impacts the MgO surface structure.

To confirm the nature of the maximum along the reaction path, an exact transition state was located starting from the geometry of the energy path maximum of the MgO(72) cluster and characterized by a frequency analysis. The transition state geometry shown in Figure 3c corresponds to an activation barrier of 0.91 eV, in excellent agreement with our approximated activation energy.

The comparison of the oxygen diffusion into neutral and cationic vacancies reveals drastic changes in the associated diffusion energy barriers. Whereas activation barriers of 2.8 to 2.9 eV were found for the neutral vacancies, these barriers reduced to around 2.2 eV for the cationic and around 0.95 eV for the dicationic vacancies. This suggests a significantly enhanced mobility of cationic vacancies on the MgO surface. The transition state geometries of neutral, cationic, and dicationic vacancies were topologically similar. However, qualitative differences in the local surface relaxation exist. As a consequence, the height of the moving oxygen atom above the MgO surface in the transition state geometry varied significantly with the vacancy charge, from 0.62 Å for the neutral vacancy to 0.50 Å for the cationic, and 0.37 Å for the dicationic vacancy (see

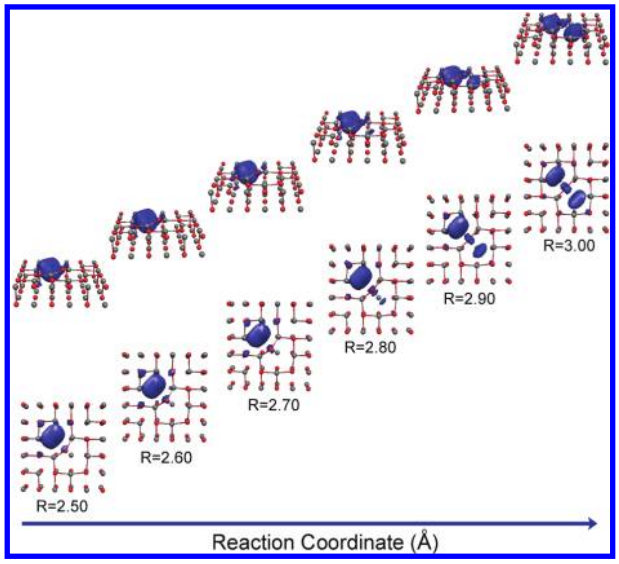

Figure 4. Perspective and top views of spin density isosurfaces (0.002 au) along the reaction path for the oxygen diffusion into a cationic oxygen vacancy. All distances are from the reference point X shown in Figure 2.

Figure 3). We note that this trend is proportional to the lowering of the corresponding activation barrier.

To investigate the effect of the surface relaxation on the energy barrier, we performed additional calculations of the energy profile with the geometry of the MgO(72) cluster frozen at the optimized geometry of the dicationic vacancy. The resulting energy barrier was found to increase to around 1.9 eV. This means that the surface relaxation is able to decrease the energy barrier by as much as 1.0 eV to the actual value of 0.91 eV for the fully relaxed case. As in the cationic vacancy case, discussed above, the electrostatic interaction between the localized positive charge and the electron-rich oxygen atoms, and the resulting surface relaxation, are responsible for lowering the oxygen diffusion barrier.

E. Charge and Spin Transfer along the Oxygen Diffusion into a Cationic Oxygen Vacancy. Given the existence of an unpaired electron in the cationic vacancy, the charge movement along the reaction path of the oxygen diffusion can be investigated by tracing the spin density. Figure 4 shows spin density isosurfaces with a spin density value of 0.002 au along the reaction coordinate R in the range of 2.5 to 3.0 Å. It can be seen from this figure that the unpaired electron remains in the vacancy until very close to the transition state despite the movement of the oxygen atom. The first indication for an electron transfer appears at 2.8 Å, only 0.2 Å before the transition state. In the next step, recorded at 2.9 Å, a more significant electron transfer is visible in Figure 4. This leads to a symmetric distribution of the unpaired electron at the transition state. These results show that the oxygen diffusion on the MgO surface is accompanied by an electron hopping mechanism. This electron hopping occurs for both cationic and neutral vacancies, which correspond respectively to one and two trapped electrons.

4. Conclusions

The transition states and activation barriers for the oxygen diffusion into neutral, cationic, and dicationic oxygen vacancies on MgO(100) surfaces have been investigated. Our results support and extend previous experimental and theoretical studies and present a new reference for these activation barriers. The charge state of the vacancy is found to decrease the oxygen diffusion energy barrier due to the attractive electrostatic interaction between the localized positive charge(s) and the electron-rich oxygen atoms, and the resulting relaxation of the surface atoms. The decrease of the oxygen diffusion barrier is accompanied by a reaction path that keeps the moving oxygen closer to the MgO surface. The oxygen diffusion was found to be localized at the MgO surface layer and is not significantly affected by relaxation of the subsurface layer or by the layer thickness. Finally, the movement of the unpaired electron during the oxygen diffusion toward a cationic oxygen vacancy was monitored by tracing the spin density along the reaction path. This analysis shows that this oxygen diffusion on MgO surfaces is accompanied by an electron hopping process.

Acknowledgment. J.U.R. and S.N.K. acknowledge support from the MURI grant from the Air Force Office of Scientific Research grant FA9550-08-1-0400. A.M.K. acknowledges support from CONACYT (60117-F), ICYTDF (PIFUTP08-87) and CIAM (107310). C.Q. acknowledges support from PAPIIT IN113509 project, and from PUNTA-UNAM project. Parts of the calculations were performed on the computational equipment of DGSCA UNAM, particularly at the supercomputer KanBalam.

References and Notes

(1) Henrich, V. E.; Cox, P. A. *The Surface Science of Metal Oxides*; Cambridge University Press: Cambridge, 1994.

(2) Tilley, R. J. D. *Principles and applications of chemical defects*; Stanley Thornes: Cheltenham, 1998.

(3) *The chemical physics of solid surfaces: Oxide surfaces*; Woodruff, P., Ed.; Elsevier: Amsterdam, 2001; Vol. 9.

(4) Kantorovich, L. N.; Holender, J. M.; Gillan, M. J. The energetics and electronic structure of defective and irregular surfaces on MgO. *Surf. Sci.* **1995**, *343* (3), 221–239.

(5) Kramer, J.; Ernst, W.; Tegenkamp, C.; Pfnür, H. Mechanism and kinetics of color center formation on epitaxial thin films of MgO. *Surf. Sci.* **2002**, *517* (1−3), 87–97.

(6) Pacchioni, G. Oxygen vacancy: The invisible agent on oxide surfaces. *ChemPhysChem* **2003**, *4* (10), 1041–1047.

(7) Wahlström, E.; Lopez, N.; Schaub, R.; Thostrup, P.; Rønnau, A.; Africh, C.; Lægsgaard, E.; Nørskov, J. K.; Besenbacher, F. Bonding of Gold Nanoclusters to Oxygen Vacancies on Rutile TiO_2(110). *Phys. Rev. Lett.* **2003**, *90* (2), 026101.

(8) Chiesa, M.; Giamello, E.; Murphy, D. M.; Pacchioni, G.; Paganini, M. C.; Soave, R.; Sojka, Z. Reductive activation of the nitrogen molecule at the surface of "electron-rich" MgO and CaO. The N_2^- surface adsorbed radical ion. *J. Phys. Chem. B* **2001**, *105* (2), 497–505.

(9) Köing, T.; Simon, G. H.; Rust, H.-P.; Pacchioni, G.; Heyde, M.; Freund, H.-J. Measuring the Charge State of the Point Defects on MgO/Ag(001). *J. Am. Chem. Soc.* **2009**, *131* (48), 17544–17545.

(10) Abbet, S.; Sanchez, A.; Heiz, U.; Schneider, W. D.; Ferrari, A. M.; Pacchioni, G.; Rosch, N. Acetylene cyclotrimerization on supported size-selected Pd_n clusters ($1 \leq n \leq 30$): one atom is enough! *J. Am. Chem. Soc.* **2000**, *122* (14), 3453–3457.

(11) Giordano, L.; Di Valentin, C.; Goniakowski, J.; Pacchioni, G. Nucleation of Pd dimers at defect sites of the MgO(100) surface". *Phys. Rev. Lett.* **2004**, *92* (9), 096105.

(12) Schaub, R.; Wahlstrom, E.; Ronnau, A.; Laegsgaard, E.; Stensgaard, I.; Besenbacher, F. Oxygen-mediated diffusion of oxygen vacancies on the TiO_2(110) surface. *Science* **2003**, *299* (5605), 377–379.

(13) Shluger, A. L.; Kantorovich, L. N.; Livshits, A. I.; Gillan, M. J. Ionic and electronic processes at ionic surfaces induced by atomic-force-microscope tips. *Phys. Rev. B* **1997**, *56* (23), 15332–15344.

(14) Sushko, P. V.; Shluger, A. L.; Catlow, C. R. A. Relative energies of surface and defect states: ab initio calculations for the MgO(001) surface. *Surf. Sci.* **2000**, *450* (3), 153–170.

(15) Coquet, R.; Hutchings, G. J.; Taylor, S. H.; Willock, D. J. Calculations on the adsorption of Au to MgO surfaces using SIESTA. *J. Mater. Chem.* **2006**, *16* (20), 1978–1988.

(16) Satoh, Y.; Kinoshita, C.; Nakai, K. Kinetic-study of Defect Clusters in the Mgo-Al_2O_3 System Under Electron-Irradiation and or Ion-Irradiation. *J. Nucl. Mater.* **1991**, *179*, 399–402.

(17) Kinoshita, C. Radiation-Induced Microstructural Change in Ceramic Materials. *J. Nucl. Mater.* **1992**, *191*, 67–74.

(18) Oishi, Y.; Ando, K.; Kurokawa, H.; Hiro, Y. Oxygen self-diffusion in MgO single-crystals. *J. Am. Ceram. Soc.* **1983**, *66* (4), C60–C62.

(19) Popov, A. I.; Monge, M. A.; Gonzalez, R.; Chen, Y.; Kotomin, E. A. Dynamics of F-center annihilation in thermochemically reduced MgO single crystals. *Solid State Commun.* **2001**, *118* (3), 163–167.

(20) Kotomin, E. A.; Kukjla, M. M.; Eglitis, R. I.; Popov, A. I. Quantum chemical simulations of the optical properties and diffusion of electron centers in MgO crystals. *Mater. Sci. Eng., B* **1996**, *37* (1−3), 212–214.

(21) Popov, A. I.; Kotomin, E. A.; Kukla, M. M. Quantum chemical calculations of the electron center diffusion in MgO crystals. *Phys. Status Solidi B* **1996**, *195* (1), 61–66.

(22) Kotomin, E. A.; Popov, A. I. Radiation-induced point defects in simple oxides. *Nucl. Instrum. Methods Phys. Res., Sect. B* **1998**, *141* (1−4), 1–15.

(23) Pacchioni, G.; Pescarmona, P. Structure and stability of oxygen vacancies on sub-surface, terraces, and low-coordinated surface sites of MgO: an ab initio study. *Surf. Sci.* **1998**, *412/413*, 657–671.

(24) Finocchi, F.; Goniakowski, J.; Noguera, C. Interaction between oxygen vacancies on MgO(100). *Phys. Rev. B* **1999**, *59* (7), 5178–5188.

(25) Carrasco, J.; Lopez, N.; Illas, F.; Freund, H.-J. Bulk and surface oxygen vacancy formation and diffusion in single crystals, ultrathin films, and metal grown oxide structures. *J. Chem. Phys.* **2006**, *125* (7), 074711−1-074711−6.

(26) Quintanar, C.; Caballero, R.; Köster, A. M. Long-range interactions in embedded ionic cluster calculations. *Int. J. Quantum Chem.* **2004**, *96* (5), 483–491.

(27) Quintanar, C.; Caballero, R.; Castaño, V. M. Adsorption of CO on the rumpled MgO(100) MgO(100): Ni, and MgO(100): Cr surfaces: A density functional approach. *Int. J. Quantum Chem.* **2005**, *102* (5), 820–828.

(28) Caballero, R.; Quintanar, C.; Köster, A. M.; Khanna, S. N.; Reveles, J. U. Structural and electronic properties of Au and Au_2 on an MgO(100) surface: A DFT cluster embedding approach. *J. Phys, Chem. C* **2008**, *112* (38), 14919–41928.

(29) Ashcroft, N. W.; Mermin, N. D. *Solid State Physics*; Holt, Rinehart and Winston: New York, 1976; p 80.

(30) Perdew, J.; Burke, K.; Ernzerhof, M. Generalized gradient approximation made simple. *Phys. Rev. Lett.* **1996**, *77* (18), 3865–3868.

(31) Köster, A. M.; Calaminici, P.; Casida, M. E.; Flores-Moreno, R.; Geudtner, G.; Goursot, A.; Heine, T.; Ipatov, A.; Janetzko, F.; del Campo, J. M.; Patchkovskii, S.; Reveles, J. U.; Salahub, D. R.; Vela, A. deMon2k, Ver. 2.3.6; The deMon Developers, Cinvestav, México (2010). Available at http://www.deMon-software.com.

(32) Mintmire, J. W.; Dunlap, B. I. Fitting the coulomb potential variationally in linear-combination-of-atomic-orbitals density-functional calculations. *Phys. Rev. A* **1982**, *25* (1), 88–95.

(33) Köster, A. M.; Reveles, J. U.; del Campo, J. M. Calculation of exchange-correlation potentials with auxiliary function densities. *J. Chem. Phys.* **2004**, *121* (8), 3417–3424.

(34) Godbout, N.; Salahub, D. R.; Andzelm, J.; Wimmer, E. Optimization of gaussian-type basis-sets for local spin-density functional calculations. 1. Boron through neon, optimization technique and validation. *Can. J. Chem.* **1992**, *70* (2), 560–571.

(35) Calaminici, P.; Janetzko, F.; Köster, A. M.; Mejia-Olvera, R.; Zuniga-Gutierrez, B. DFT Optimized Basis Sets for Gradient Corrected Functionals: 3d Transition Metal Systems. *J. Chem. Phys.* **2007**, *126* (4), 044108.

(36) Reveles, J. U.; Köster, A. M. Geometry optimization in density functional methods. *J. Comput. Chem.* **2004**, *25* (9), 1109–1116.

(37) Reveles, J. U.; Khanna, S. N.; Köster, A. M. Equivalent delocalized internal coordinates. *J. Mol. Struct. (THEOCHEM)* **2006**, *762* (1−3), 171–178.

(38) del Campo, J. M.; Köster, A. M. A Hierarchical Transition State Search Algorithm. *J. Chem. Phys.* **2008**, *129* (2), 024107.

(39) Ferrari, A. M.; Pacchioni, G. Electronic Structure of F and V centers of the MgO Surface. *J. Phys. Chem.* **1995**, *99* (46), 17010–17018.

JP1040184